Models and Molecular Orbital Semiempirical Calculations in the Study of the Spectroscopic Properties of Bovine Serum Amine Oxidase Quinone Cofactor†

Mario Bossa, Giorgio O. Morpurgo,* and Laura Morpurgo‡

Department of Chemistry and CNR Centre of Molecular Biology c/o Department of Biochemical Sciences, University of Rome "La Sapienza", P.le A. Moro 5, 00185 Rome, Italy

Received December 6, 1993®

ABSTRACT: The electronic properties of 2,4,5-trihydroxyphenylalanine quinone (TPQ), the cofactor of bovine serum amine oxidase [Janes, S. M., Mu, D., Wemmer, D., Smith, A. J., Kaur, S., Maltby, D., Burlingame, A. L., & Klinman, J. P. (1990) *Science 248*, 981–987], and some adducts with hydrazines were investigated by means of low-molecular-weight models and semiempirical molecular orbital calculation methods. The enzyme visible band was assigned to the first $\pi \rightarrow \pi^*$ transition of the cofactor in *p*-quinonic form, with the C-4 hydroxyl ionized and hydrogen bonded either to a water molecule or to a basic protein residue. The spectra of the protein adducts with some substituted hydrazines were well accounted for by assuming the inhibitor bound to the C-5 carbonyl, usually in azo form. The adduct with the unsubstituted hydrazine was instead assigned an *o*-quinone hydrazone form, stabilized by an internal hydrogen bond between the amino group and the *ortho* carbonyl oxygen, a larger electron delocalization, and formation of a hydrogen bond at the C-6 ionized hydroxyl. On the basis of these assignments, the reaction of the protein with benzylhydrazine [Morpurgo, L., Agostinelli, E., Muccigrosso, J., Martini, F., Mondovi, B., & Avigliano, L. (1989) *Biochem. J. 260*, 19–25] was rewritten. All examined electronic transitions, though highly sensitive to cofactor ionization and hydrogen bonding, could be accounted for without introducing perturbations due to copper. This confirms that copper is not within bonding distance of the oxidized cofactor.

The copper-containing bovine serum amine oxidase (BSAO, EC 1.4.3.6), which catalyzes the oxidative deamination of primary amines, was shown to contain, as a cofactor, an oxidized tyrosine, the 2,4,5-trihydroxyphenylalanine quinone (TPQ) (Janes *et al.*, 1990). This very reactive compound could not be isolated from the enzyme in the free form but only as a phenylhydrazone adduct in a pentapeptide obtained upon enzymatic hydrolysis (Janes *et al.*, 1990). It was indirectly identified in the intact protein by resonance Raman spectroscopy, since a peculiar set of vibrational modes allowed to distinguish TPQ from related coenzymes such as pyrroloquinoline quinone and tryptophantryptophyl quinone (Sanders-Loehr *et al.*, 1991).

A variety of spectroscopic data is available on the amine oxidase cofactor, mostly derived from studies of the reactions with hydrazines, which inhibit the enzyme activity forming stable Shiff's adducts (Morpurgo *et al.*, 1988, 1992) or act as pseudosubstrates giving rise to multistep reactions (Morpurgo *et al.*, 1989). The correct identification of the species is important since it may provide information on TPQ electronic structure, about which little is known. Previous studies referred to either a "carbonyl cofactor" (Pettersson, 1985) or pyrroloquinoline quinone (Ameyama *et al.*, 1984; Lobenstein-Verbeek *et al.*, 1984) as the cofactor. In principle, several isomeric forms are possible for TPQ and its hydrazine adducts, such as *o*-/*p*-quinone and hydrazone/azo forms. The analysis of spectroscopic data with the aid of molecular orbital (MO) theory calculations was initiated in the hope to gain a deeper insight into the cofactor electronic and basic structural features, on which chemical properties ultimately reside. A preliminary study of quinonoid cofactors and their phenylhydrazine adducts was already carried out (Bossa *et al.*, 1992) using the MO calculation method in the Pariser–Parr–Pople (PPP) approximation and the parametrization of Morozov and Chekov (1989), which successfully analyzed the spectra of vitamin B_6 and its analogues. The conclusion was reached that pyrroloquinoline quinone is not the cofactor of amine oxidase and other quinoproteins absorbing around 480 nm ($\epsilon = 3500\ M^{-1}\ cm^{-1}$), since it was not expected to display $\pi \rightarrow \pi^*$ transitions at wavelengths >400 nm. As far as a TPQ spectrum was concerned, the lowest energy $\pi \rightarrow \pi^*$ transition was calculated at 425 nm. In the present work, previous results were refined and the study was extended to hydrazine derivatives. The PPP method was coupled to the Austin Model 1 (AM1) method (Dewar *et al.*, 1985) when optimization of the molecular geometry was required. Although PPP and AM1 have both undergone extensive checking and validation, their reliability was first tested on simple quinonoid molecules related to the cofactor, such as substituted *p*-quinones.

Although 2,4,5-trihydroxybenzyl hydantoin quinone (Janes *et al.*, 1990; Mure & Klinman, 1993) and the quinone obtained by oxidation of trihydroxyphenethylamine (Pedersen *et al.*, 1992) were employed as good TPQ models, the use of the commercially available 2,5-dihydroxy-1,4-benzoquinone (Figure 1) was preferred in this work. The lack of free amino groups in this molecule turned out to be very convenient from both the experimental and theoretical point of view.

The presence of copper was disregarded in calculations since it does not appear to influence the coenzyme electronic properties. Much evidence is available on this matter: (i) the optical spectra of native BSAO and the phenylhydrazine adduct are not modified by either copper removal or copper substitution with cobalt or nickel (Suzuki *et al.*, 1983); (ii) the spectra of hydrazine and benzylhydrazine adducts are unaffected by copper substitution with cobalt (Morpurgo *et*

† The research was in part supported by the CNR, Contract CTB 92.00466.03.

* Correspondence address: Department of Chemistry, University of Rome "La Sapienza", P.le A. Moro 5, 00185 Rome, Italy.

‡ CNR Centre of Molecular Biology c/o Department of Biochemical Sciences.

® Abstract published in *Advance ACS Abstracts*, March 1, 1994.

0006-2960/94/0433-4425$04.50/0

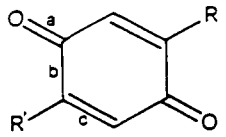

R = R' = H	1,4-benzoquinone: a = 1.23 Å; b = 1.49 Å; C = 1.32 Å
R = R' = OH	2,5-dihydroxy-1,4-benzoquinone
R = alanyl, R' = OH	TPQ
R = -CH_2-hydanthoin, R' = OH	trihydroxybenzylhydanthoin quinone
R = -CH_2-CH_2-NH_2, R' = OH	trihydroxyphenethylamine quinone

FIGURE 1: Substituted 1,4-benzoquinones. Bond lengths and angles were taken from *Tables of Interatomic Distances* (1958) Special Publication no. 11, p 194, The Chemical Society, London.

al., 1990); (iii) the spectra of model molecules such as free TPQ hydantoin (Janes *et al.*, 1990) and trihydroxyphenethylamine quinone (Pedersen *et al.*, 1992) display a band at 480 nm as BSAO; and (iv) identical resonance Raman spectra were recorded on native BSAO, the TPQ-containing pentapeptide, and TPQ hydantoin after derivatization with phenylhydrazine or (*p*-nitrophenyl)hydrazine (Brown *et al.*, 1991).

MATERIALS AND METHODS

Materials. 2,5-Dihydroxy-1,4-benzoquinone, 2,4,5-trihydroxyphenethylamine, and *N*-methylimidazole were purchased from Aldrich-Chemie. Imidazole was a BDH product. Pyridine and 4-methylpyridine were C. Erba RP reagents. Phenylhydrazine, 3,4-dimethylpyridine, 4-(dimethylamino)-pyridine, and all solvents, including the deuterated solvents employed in NMR experiments, were Merck products.

Instrumentation. Visible and near-UV absorption spectra were recorded on a Lambda-9 Perkin-Elmer spectrophotometer. ^{1}H-NMR spectra were obtained using a Brucker WP80 spectrometer. IR spectra were recorded on a Perkin-Elmer FT-IR 1700X spectrometer.

Sample Preparation. Stock solutions of 20 mM trihydroxyphenethylamine chloridrate in deaerated methanol were freshly prepared and kept under Ar. Aliquots (30–90 μL) were withdrawn with an air-tight microsyringe through a serum cap and added to an appropriate volume of air-equilibrated methanol or buffer. The oxidation to the quinone occurred within minutes, and then stable spectrophotometric readings were obtained. At neutral pH, the spectrum was similar to that reported in literature (Pedersen *et al.*, 1992). A rapid decay reaction prevented the accurate measurement of the quinone spectrum in 0.1 N NaOH. No particular precautions were required by the manipulation of dihydroxybenzoquinone, the spectra of which were very similar to those recorded a long time ago by Schwarzenbach and Suter (1941).

Solid adducts between dihydroxybenzoquinone and bases were prepared by adding a concentrated solution of the base to a stirred solution of the quinone in the minimum volume of an appropriate solvent. Methanol was used for all bases except *N*-methylimidazole and (dimethylamino)pyridine for which acetonitrile was used. A slight base excess over the 1:1 stoichiometric ratio was used in all cases except (dimethylamino)pyridine, which was added in a 3:1 ratio. The red crystalline products were separated by vacuum filtration, washed first with the same solvent used in the preparation and then with ethyl ether, and dried *in vacuo*. Element analyses and the formula assigned to the adducts are reported in Table 1.

Table 1: Element Analysis and Formula of Solid Adducts of Bases with Dihydroxybenzoquinone

formula[a]	experimental C	H	N	calculated C	H	N
Q_2·pyridine	56.99	3.65	3.79	56.83	3.62	3.90
Q·methylpyridine	61.75	4.61	5.73	61.80	4.72	6.01
Q·dimethylpyridine	63.18	5.28	5.45	63.16	5.26	5.67
Q·imidazole	52.45	3.97	3.52	51.92	3.85	13.46
Q_3·(methylimidazole)$_2$	53.97	4.10	9.36	53.40	4.11	9.58
Q_3·[(dimethylamino)pyridine]$_2$	57.95	5.05	8.53	57.80	4.82	8.43

[a] Q = dihydroxybenzoquinone.

Table 2: Parameters Employed in PPP Calculations

	$-I_\mu$	$\gamma_{\mu\mu}$	Z_σ	$-A_{\mu\nu}$	$-B_{\mu\nu}$
C	11.16	11.13	1.00	2.05	0.51
N^+	22.60	16.76	1.50	2.23	0.53
N_{arom}	14.12	12.34	1.00	2.23	0.53
—N=	15.12	12.34	1.00	2.23	0.53
=O	17.70	15.23	1.00	2.45	0.56
—O—	32.60	21.53	2.00	2.45	0.56
—OH···X[a]	25.70	18.30	2.00	2.45	0.56
$-O^-$	19.80	15.23	2.00	2.45	0.56
Cl	24.02	11.27	2.00	1.859	0.00
Br[a]	19.10	7.30	2.00	1.859	0.00

[a] See also text.

1. The deuterated *N*-methylimidazole adduct for IR measurements was obtained by dissolving the quinone in deuterated methanol. The solvent was then evaporated. After several cycles of solution/solvent evaporation, *N*-methylimidazole was added, and some drops of the deuterated solution were left to evaporate on a NaCl disk in a vacuum desiccator.

The dihydroxybenzoquinone phenylhydrazone was prepared by mixing 5 mmol of quinone with 5 mmol of phenylhydrazine chloridrate in 60 mL of methanol containing 0.1 mL of 0.1 N HCl. Evaporation of the solvent to about one-half the initial volume led to precipitation of the crude adduct. Dark brown-red crystals were obtained on recrystallization from 95% ethanol. Anal. ($C_{12}H_{10}N_2O_3 \cdot {}^1/_2H_2O$) C calcd 60.25, found 60.78; H, calcd 4.60, found 4.54; N, calcd 11.72, found 11.82. The presence of H_2O was confirmed by the IR spectrum.

Calculation Methods. The PPP method, the simplest ZDO-SCF method, was primarily developed to calculate the electronic spectra of planar, conjugated organic molecules. It only deals with π-electron systems and is then unsuited to reproduce the portions of the spectra due to $n \rightarrow \pi^*$ transitions. The method was chosen for its simplicity and reliability, given a suitable parametrization. The semiempirical parameters used in the present calculations, namely the atomic ionization potential (I_μ), the one-center electronic repulsion integral ($\gamma_{\mu\mu}$), the charges of the σ-electron core of the μth atom (Z_σ), and the parameters $A_{\mu\nu}$ and $B_{\mu\nu}$, which are required to calculate the two-center core integrals ($\beta_{\mu\nu}$), were taken from the work of Morozov and Chekov (1989) and are reported in Table 2. The only exceptions are the parameters used for O^- (*vide infra*) and Cl^-, for which the values reported by Tinland (1968) were found to give more satisfactory results. $\beta_{C\text{-}Br}$ was equalized to $\beta_{C\text{-}Cl}$.

Geometry optimization was obtained by means of AM1, using MOPAC (A General Molecular Orbital Package, QCPE 455, version 4.10). The method provides a reliable evaluation of hydrogen-bonded systems (Dewar *et al.*, 1985; Coitiño & Ventura, 1989; Ventura *et al.*, 1989; Dannenberg & Evlet, 1992).

Table 3: Absorption Bands of Dihydroxybenzoquinone and Hydroxyphenethylamine Quinone

conditions	experimental λ (nm)	experimental ε (M^{-1} cm^{-1})	calculated λ (nm)	calculated ε (M^{-1} cm^{-1})
	Dihydroxybenzoquinone			
methanol	286	21000	296	22100
	395	242	386	0
pH 1.8	283	17000		
	400	248		
pH 5.6	203	22200	220	18470
	228	2800 (sh)		
	312	17300	317	17900
	489	470	474	1450
pH 8.0	203	22200	213	43550
	230	5280 (sh)	231	7780
	323	20150	345	19540
	504	240	485	370
	Trihydroxyphenethylamine Quinone			
0.1 N H_2SO_4	263	16000	262	19000
	384	840	372	3130
pH 7.2	211	22800	219	34300
	268	10500	268	7500
	486	2080	473	3500
0.1 N NaOH	285	9560		
	478	1850		

RESULTS

Solvent Dependence of Dihydroxybenzoquinone Spectra. Dihydroxybenzoquinone is a diprotic acid (K_1 = 5.18, K_2 = 2.71; Schwarzenbach & Suter, 1941). As reported in literature (Braude, 1945), the fully protonated species (in 0.1 N H_2SO_4) showed bands at 283 and 400 nm (Table 3). At higher pH, the visible band was shifted to 485 nm and its intensity increased, reaching a maximum (820 M^{-1} cm^{-1}) at pH 4.30, and then decreased again when the dianionic species started to form. The latter species showed a longest wavelength band at 504 nm and a near-UV band at 323 nm (Table 3).

The spectrum of the fully protonated species was also measured in nonaqueous solvents such as chloroform, dichloromethane, and methanol. On addition of a base with pK_a exceeding that of dihydroxybenzoquinone by at least 2 units, such as pyridine or imidazole, the low-energy transition was shifted from 400 to 485 nm. The Job's plots of Figure 2, measured in methanol or CH_2Cl_2, show that the 485-nm band was produced by equilibrium reactions leading to prevalent formation of a 1:1 species (plus some 2:1 quinone/base product with bases of low pK_a). At fixed ratios of quinone and base, the intensity of the 485-nm band was, in general, higher, the higher the base pK_a.

The absorbance vs pK_a plot gave rise to an S-shaped curve at a proper quinone/base ratio, which depended on the solvent used. A 1:1 ratio was sufficient in methanol (Figure 3), while a 10-fold base excess was required in dimethylformamide. From equimolar dihydroxybenzoquinone and base solutions, 2:1, 1.5:1, or 1:1 adducts precipitated (Table 1). These stoichiometries, which depend on the base used, suggest that polymeric species were formed.

^{1}H-NMR Spectra. The ^{1}H-NMR spectra of the bases in deuterated methanol solution showed that the signals of the protons *ortho* to the nitrogen underwent a downfield shift on interaction with dihydroxybenzoquinone. The C-2 proton signal of imidazole was shifted from 7.66 to 8.50 ppm, while the C-4 and C-5 doublet was shifted from 7.04 and 7.05 to 7.41 ppm. The corresponding shifts for *N*-methylimidazole were from 7.56 to 7.86 ppm and from 6.94 and 7.05 ppm to

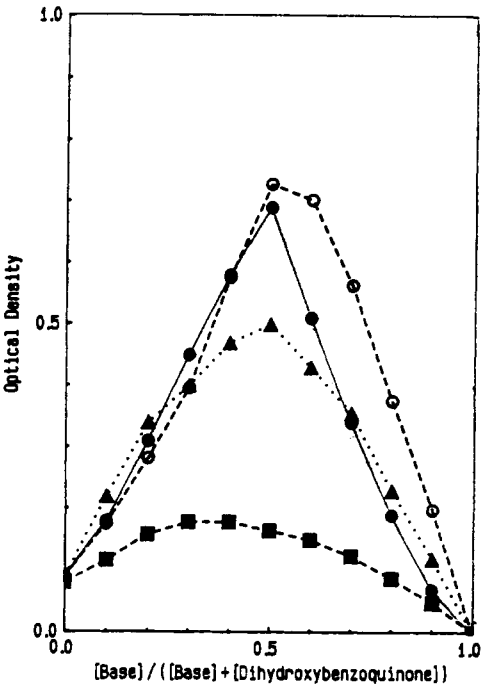

FIGURE 2: Job's plots for dihydroxybenzoquinone reaction with N-bases. In methanol: imidazole (▲), 4-methylpyridine (■), and (dimethylamino)pyridine (●). In CH_2Cl_2: (dimethylamino)pyridine (○). Optical density was recorded at 485 nm; 1.0 mM solutions were used.

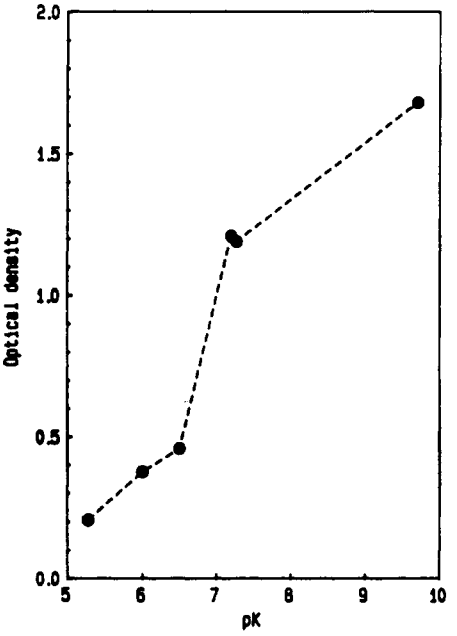

FIGURE 3: Adduct formation between dihydroxybenzoquinone and N-bases as a function of the base pK_a. Optical density at 485 nm of 2.0 mM quinone and 2 mM N-base in methanol.

7.08 and 7.17 ppm. The *ortho* proton signals of 3,4-dimethylpyridine, a doublet at 8.16 and 8.22 ppm, were shifted to 8.29 and 8.36 ppm, while the doublet at 7.15 and 7.21 ppm, due to the *meta* proton, was shifted to 7.40 and 7.47 ppm. The proton signals of the -inium ions were found at a much lower field: at 8.86 ppm the C-2 proton and at 7.56 ppm the C-4 and C-5 proton signals of the imidazolinium ion, at 8.81 and 7.54 ppm the corresponding signals of the *N*-methylimidazolium ions, and at 8.60 and 8.53 ppm the *ortho* proton doublet and at 7.87 and 7.94 ppm the *meta* proton doublet of the 3,4-dimethylpyridinium ion. These perturbations show that

Table 4: Dependence of ν(OH) and ν(CO) on the Base pK_a in Solid Dihydroxybenzoquinone–N-Base Adducts

base	pK_a	ν(OH) (cm^{-1})	ν(CO) (cm^{-1})	
pyridine	5.28	3228	1662	1632
4-methylpyridine	6.00	3206	1657	1622
3,4-dimethylpyridine	6.50	3163	1651	1603
imidazole	7.20	3131	1636	1582
N-methylimidazole	7.27	3199	1662	1608
4-(dimethylamino)pyridine	9.71	3159	1646	1598

quinone and bases interact, most likely forming hydrogen-bonded adducts.

IR Spectra of Solid Dihydroxybenzoquinone–Base Adducts. The limited solubility of dihydroxybenzoquinone–base adducts prevented IR measurements in solution. Such spectra were therefore recorded only on solid compounds. The IR spectrum of dihydroxybenzoquinone shows a peak at 3298 cm^{-1}, which was assigned to ν(OH) stretching of the inter- and intramolecular OH···O bond. The peak at 1614 cm^{-1}, with a subband at 1647 cm^{-1}, was assigned to the CO stretching vibration (Nakamoto *et al.*, 1955). The OH peak was preserved in the adducts with bases, but it was shifted to increasingly lower frequencies, the higher the base pK_a. The trend was abruptly interrupted (Table 4) in the *N*-methylimidazole and (dimethylamino)pyridine derivatives. The CO stretching bands, which were split in the adducts, followed a similar trend. Also, a new band system was formed, consisting of a broad absorbance in the 3000–2000-cm^{-1} range overlayed by several submaxima due to CH stretching modes. The intensity of the broad band was maximum in the *N*-methylimidazole adduct. In the (dimethylamino)pyridine adduct, it showed some decrease because an absorbance contribution at about 2600 cm^{-1} disappeared. On deuteration, the band at 3159 cm^{-1} of the (dimethylamino)pyridine adduct (Table 4) disappeared and the broad band below 3000 cm^{-1} became barely detectable, showing that they were both proton dependent.

PPP Calculations on Quinones. The structural parameters obtained from the X-ray-determined geometry of 1,4-benzoquinone are shown in Figure 1. Same bond lengths and angles were used for substituted quinones when the structure was not available, while standard values from the international tables were employed for the substituents. The aromatic character of the benzoquinone is very limited, as inferred from the long distances between the CO carbons and the adjacent carbon atoms (1.49 Å). The molecule can be considered to consist of two C=O groups linked by almost single bonds to two ethylene groups. To take into account this peculiarity, the two-center core integrals $\beta_{\mu\nu}$ were fixed at the maximum value when the atoms were linked by a double bond and at the minimum when the atoms were linked by an almost single bond, and the calculation was not iterated, at variance from the previous work (Bossa *et al.*, 1992). The adjustment of the integrals by iteration was only allowed for molecules having a number of possible resonance structures, such as the undissociated, monoanionic, and dianionic dihydroxybenzoquinones, which will be analyzed in the next section. The transition energies obtained for benzoquinone and a number of substituted derivatives are reported in Table 5. The plot of experimental (Braude, 1945) vs predicted energies shows a very good linear correlation (Figure 4). Band intensities were also reasonably reproduced.

PPP Calculations of Hydroxybenzoquinone Electronic Transitions. The two transitions at 283 and 400 nm of undissociated dihydroxybenzoquinone were well reproduced by calculations. They are assigned to singlet → singlet, $\pi \rightarrow \pi^*$ transitions. The rather intense band at higher energy is theoretically allowed, while the other, of much lower intensity, is a symmetry-forbidden transition. Following the Grunwald (1965) scheme for acid dissociation, the aquated dihydroxybenzoquinone monoanion was assumed to be formed according to the simplified reaction of Scheme 1.

Table 5: Absorption Spectra of Substituted Benzoquinones[a]

substituent	experimental λ (nm)	experimental ε (M^{-1} cm^{-1})	calculated λ (nm)	calculated ε (M^{-1} cm^{-1})
	245	23000	257	27300
	281	470	303	0
Cl	258	19600	262	23550
	323	815	333	1900
2,6-diCl	275	22100	279	23800
	341	635	349	175
2,5-diCl	274	23000	278	24900
	330	295	248	0
triCl	281	20000	284	22400
	364	510	377	977
tetraCl	282	21400	298	22700
	292	23800		
	372	280	396	0
Br	258	12000	263	22000
	338	1070	346	2700
2,6-diBr	282	13700	289	22100
	292	15000		
	362	810	363	384
2,5-diBr	282	12000	288	23800
	291	12300		
	351	240	362	0
triBr	301	12500	296	20700
	385	665	401	1240
tetraBr	314	17500	315	21300
	398	300	423	0

[a] Experimental values were taken from Braude (1945).

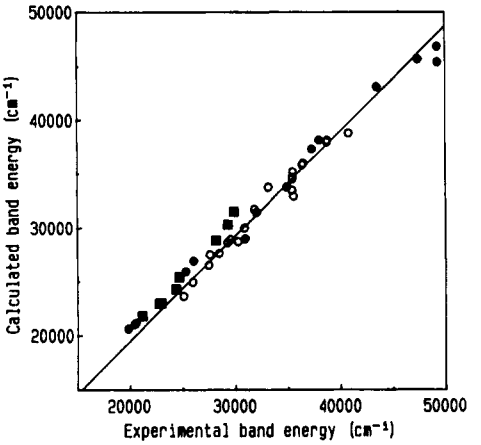

FIGURE 4: Reliability of the PPP calculation method. Open circles refer to benzoquinones (Table 5), filled circles to dihydroxybenzoquinone and hydroxyphenethylamine quinone (Table 3), and filled squares to the adducts of dihydroxybenzoquinone and bovine serum amine oxidase with hydrazines (Table 6).

Scheme 1

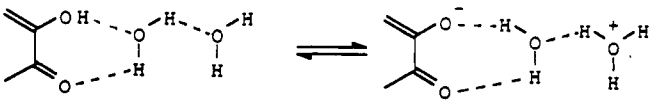

The AM1-optimized geometry of the anion (Bossa *et al.*, 1993) shows that the O$^-$···HO group forms the longest side of an irregular trapezium, with R(O$^-$···O) = 3.16 Å and R(O$^-$···H) = 2.20 Å, the opposite side of which is formed by the other water proton and the C=O oxygen. In performing

Table 6: Absorption Bands of Hydrazine Adducts of BSAO and Dihydroxybenzoquinone

hydrazine	experimental λ (nm)	experimental ε (M^{-1} cm^{-1})	calculated λ (nm)	calculated ε (M^{-1} cm^{-1})
	Dihydroxybenzoquinone			
phenylhydrazine)	438	24200	436	24270
(in $CHCl_3$	341	16000	330	14600
	268	14000	270	4700
	BSAO			
phenylhydrazine·H^+ [a]	447	42000	447	25000
			349	4300
			280	7900
phenylhydrazine[b]	434		435	41000
			334	2900
			273	4000
benzylhydrazine·H^+ [c]	470	4000 (sh)	472	3300
	405	22000	392	22900
benzylhydrazine[c]	355	12000	347	9000
			296	12000
hydrazine[c]	410	8000	412	6000
	335	20000	317	18000

[a] Morpurgo *et al.* (1992). [b] Pentapeptide adduct (Janes *et al.*, 1990). [c] Morpurgo *et al.* (1989).

the PPP calculations, the hydrogen-bond formation was accounted for by changing the oxygen ionization potential and the one-center repulsion integral. A reasonable choice for these parameters seemed to be the average between the corresponding values for OH and O^- [see Table 2 and Bossa *et al.* (1992)]. In this way, the agreement between theoretical and experimental electron-transition energies became quite satisfactory (Table 3). Using the values for fully ionized O^-, a much higher wavelength (≈650 nm) was obtained for the transition. The same applies to the anion of trihydroxyphenethylamine quinone, which was present in neutral or basic solutions. It must be noted that the lowest energy band of this compound was found at 480 nm in methanol also in the absence of bases, most probably because an intermolecular hydrogen bond was formed with the amino group of another molecule. Upon dissociation of the second dihydrozybenzoquinone hydroxyl, the lowest $\pi \rightarrow \pi^*$ band shifted to 504 nm. To fit this spectrum, different parameters had to be used in calculations for the two oxygen ions, that of the free and solvated anion, respectively.

Adducts with Hydrazines. In performing PPP calculations concerning the phenylhydrazine adduct of dihydroxybenzoquinone, the azo form was considered, since the IR spectrum of the solid derivative lacked any CO stretching band and showed a very weak peak at 1645 cm^{-1}, most likely due to ν(N=N). The optical spectrum measured in $CHCl_3$ was exceptionally well reproduced (Table 6). However, calculations on a similar azo form for the TPQ adduct with phenylhydrazine bound to the C-5 carbonyl gave lower values for wavelength and intensity of the higher energy band than the experimentally determined ones. A much better agreement was obtained by assuming either the azo group to be protonated, as previously suggested (Morpurgo *et al.*, 1992), or the C-2 hydroxyl to be hydrogen bonded. In the latter hypothesis, the transition at 434 nm of the peptidized protein adduct (Janes *et al.*, 1990) was satisfactorily matched (Table 6).

Other hydrazines form with BSAO unstable adducts (Hucko-Haas & Reed, 1970). In the formation and decay of the adduct with benzylhydrazine, three spectroscopically different species were detected, respectively characterized by

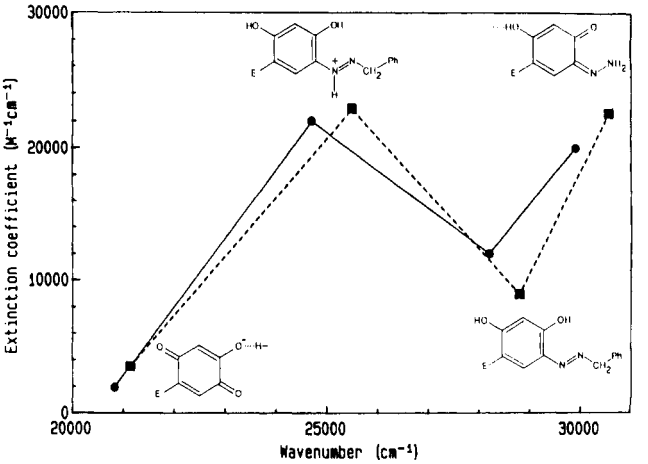

FIGURE 5: Comparison of experimental (●) and calculated (■) absorption bands of the adducts formed in the reaction of BSAO with benzylhydrazine. The highest intensity band was selected for each species.

bands at 405, 355, and 335 nm plus a shoulder at 400 nm (Morpurgo *et al.*, 1989). The last compound is a hydrazine adduct since it was also prepared by direct interaction of native amine oxidase with hydrazine. The results of PPP calculations which better explain the spectroscopic data are reported in Table 6. The electronic transitions of the first two intermediates were accurately reproduced by PPP calculations as the C-5-protonated azo derivative and the neutral azo derivative, respectively. In the case of the final hydrazine adduct, a good agreement between experimental and calculated transitions was obtained by assuming the C-5 hydrazone of TPQ to be in *o*-quinone form. AM1 calculations supported this hypothesis, showing that this form is stabilized by a larger electron delocalization and the formation of an intramolecular hydrogen bond between one of the hydrazone NH_2 protons and the *ortho* C=O oxygen. A still better result was obtained by employing reduced parameters for the hydroxyl at C-2, which amounts to ionization and formation of a hydrogen bond (Table 6). The good correlation of band position and intensity between the real system and the model is shown in Figure 5.

DISCUSSION

Hydrogen Bonding of Dihydroxybenzoquinone. Job's plots in Figure 2 show that the main product of the interaction between benzoquinone and bases is a 1:1 adduct absorbing at 485 nm. The deshielding in NMR spectra of the protons *ortho* to the bases' nitrogen, upon adduct formation with the quinone, suggests that hydrogen-bonded complexes were formed (Vinogradov & Linnel, 1971). The same result was obtained from AM1 calculations concerning the optimized geometry of the benzoquinone–pyridine adduct (Bossa *et al.*, 1993). Similar complexes are extensively described in literature, some examples being the adducts of carboxylic acids with imidazole and other bases (Lindemann & Zundel, 1977a), of phenols with substituted anilines and pyridines (Dierckx *et al.*, 1965), of carboxylic and polyglutamic acids with bases (Lindemann & Zundel, 1977b), and of *p*-nitrophenol with amines (Scott *et al.*, 1965). Specifically, the latter compounds give rise in nonaqueous solvent to tautomeric proton-transfer equilibria between the hydrogen-bonded undissociated phenol, absorbing at 315 nm, and the hydrogen-bonded phenolate anion absorbing at 400 nm.

$$-OH\cdots N^- \rightleftharpoons -O^-\cdots H^+N-$$

Scheme 2

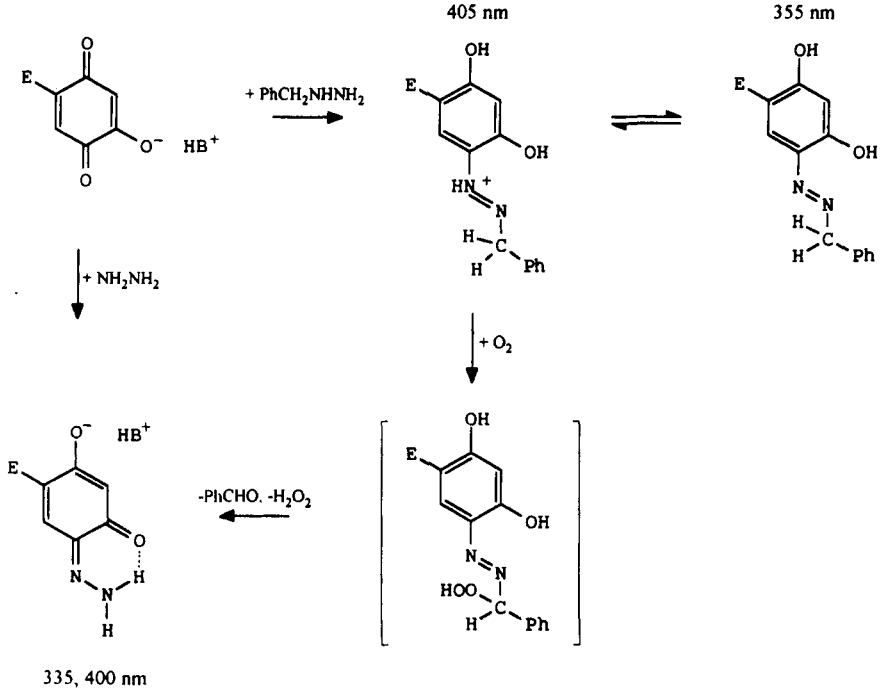

In the present case, the band at 485 nm is assigned to the 2,5-dihydroxy-*p*-benzoquinone monoanion in a proton-transfer-to-N-base adduct. The above tautomeric equilibrium implies the presence of a double minimum in the potential energy function of the proton (Schuster *et al.*, 1976). The position of the equilibrium depends on the relative heights of the two minima, which are in turn sensitive to both the relative strength of donor and acceptor and to the solvent. Then, for a given proton donor in a given solvent, the equilibrium position is expected to depend on the pK_a of the protonated N-base according to a curve recalling a titration curve. This was actually found (Figure 3) by plotting the 485-nm band intensity vs N-bases pK_a. The 50% proton transfer at $pK_a = 7$ indicates the conditions of easiest hydrogen-bond polarizability in methanol.

These conclusions are supported by the examination of the IR spectra of the red solid dihydroxybenzoquinone adducts with bases. Two band systems due to OH stretching are to be considered. The first one is the 3298-cm^{-1} peak in the unreacted quinone, arising from the stretching of the OH involved in hydrogen bonds with carbonyl oxygen atoms (Holmgren *et al.*, 1988). This band was shifted in the adducts, and the shift correlated with the base pK_a, with the exception of *N*-methylimidazole and (dimethylamino)pyridine. It is assigned to the quinone moiety which is not directly bound to the N-base and which is probably modified by polymerization in the two latter adducts (see formulas in Table 2). The other band system, a *continuum* between 2000 and 3000 cm^{-1}, was only present in the spectrum of the adducts and is thus related to the strong hydrogen bond between quinone and base. The continuum, most relevant in the *N*-methylimidazole adduct, shows the presence of a highly polarizable hydrogen bond (Nakamoto *et al.*, 1955). This assignment is supported by the increased splitting (Table 4) of the CO stretching band in the adducts with respect to the unreacted quinone (Holmgren *et al.*, 1988).

The identity of dihydroxybenzoquinone spectra in slightly acidic water solutions, where the monoanion is present (Schwarzenbach & Suter, 1945), and in nondissociating solvents, such as CH_2Cl_2 and $CHCl_3$ in the presence of N-bases, implies that a similar chromophore, with similar charge distribution on the atoms, was present in the different experimental conditions. This requires the formation in the two cases of a similar hydrogen bond between the oxo group and either a water molecule or a N-base. The use of intermediate parameters (between those for $-O^-$ and –OH) for this oxygen in the PPP calculation of spectral transitions is then legitimated on both theoretical and practical grounds.

The spectrum of trihydroxyphenethylamine quinone was well reproduced by calculations by substituting the undissociated –OH of dihydroxybenzoquinone monoanion with a methylene group. This means that the $-O^-$ group of this molecule is also hydrogen bonded to a water molecule. The same bond with water or with a basic protein residue is very likely also formed by TPQ in BSAO, since its visible band occurs at the same wavelength.

Adducts with Hydrazines. On the basis of the formulas assigned by PPP calculations to the adducts of BSAO with benzylhydrazine, the previously proposed reaction (Morpurgo *et al.*, 1989) can be rewritten according to Scheme 2. The 405-nm absorbing species, assigned to a protonated azo adduct, is more likely to react with oxygen than the 355-nm absorbing one. This species, which was only observed in deaerated solutions, probably lies off the reaction path, as do the intermediates recently evidenced in the reaction of BSAO with *para* substituted benzylamines (Hartman *et al.*, 1993). An *o*-quinone form, stabilized by an internal hydrogen bond between NH_2 and the *ortho* carbonyl oxygen and by a further hydrogen bond of the ionized hydroxyl at C-6, is assigned to the final reaction product. This explains the relatively high stability of the BSAO–hydrazine adduct. The formation of α-azohydroperoxides from the corresponding phenylhydrazones and oxygen in enzyme-catalyzed reactions was also reported for lipoxygenases (Galey *et al.*, 1988) and peroxidases (Mahy *et al.*, 1993).

CONCLUSIONS

The investigation on the electronic properties of TPQ, which was carried out by combining model studies and semiempirical

calculation methods, shows that the BSAO spectrum is less "shapeless" than previously thought (Duine, 1991). The band at 480 nm (ϵ = 3500 M^{-1} cm^{-1}) was assigned to the first $\pi \rightarrow \pi^*$ transition of TPQ monoanion, in which O^- and the adjacent *p*-quinone carbonyl oxygen are hydrogen bonded either to a water molecule or to a protein basic group.

A new structure was assigned to the intermediates in BSAO-catalyzed oxidation of benzylhydrazine, allowing reformulation of the reaction mechanism. The hydrogen bond of TPQ monoanion was formed in a different position in the adduct with hydrazine and was no longer present in azo adducts. The change of hydrogen-bond pattern may trigger the inhibition of the second BSAO functional unit, as observed in several cases (Morpurgo *et al.*, 1992).

^{19}F-NMR (Williams *et al.*, 1986) and fluorescence measurements (Lamkin *et al.*, 1988), carried out on amine oxidase from pig plasma, concluded that copper is not within bonding distance of the cofactor. The same conclusion is reached here, that copper, though catalytically competent, is not bound to TPQ, at least in oxidized BSAO. The spectrum of the native protein and several adducts could be assigned by means of PPP calculations, though the copper presence was ignored. Otherwise, it would certainly affect the π-system, which is very sensitive to the surroundings.

In a recent study of the BSAO cofactor by means of models, titration experiments showed that TPQ pK_a is 1 unit lower in the protein than in free TPQ–hydantoin (Mure & Klinman, 1993). The difference was proposed to arise from an interaction of TPQ either with copper or with a positively charged protein residue, the former hypothesis being preferred by the authors. The present paper on one side confirms that TPQ is present in BSAO in anionic form and on the other provides evidence that the second hypothesis is the more likely one. It may be interesting to note that evidence was presented for a functional role for histidine in lysyl oxidase catalysis (Gacheru *et al.*, 1988).

ACKNOWLEDGMENT

We wish to thank Dr. G. Frachey for assistance in obtaining NMR spectra.

REFERENCES

Ameyama, M., Hayasashi, M., Matsushita, K., Shinagawa, E., & Adachi, O. (1984) *Agric. Biol. Chem. 48*, 561–565.
Bossa, M., Gelsomino, I., Morpurgo, G. O., Morpurgo, L., & Talamo, A. (1992) *THEOCHEM 254*, 533–538.
Bossa, M., Brahimi, M., Morpurgo, G. O., & Morpurgo, L. (1993) *THEOCHEM 287*, 269–273.
Braude, E. (1945) *J. Chem. Soc.* 490–497.
Brown, D. E., McGuirl, M. A., Dooley, D. M., Janes, S. M., Mu, D., & Klinman, J. P. (1991) *J. Biol. Chem. 266*, 4049–4051.
Coitiño, E. L., & Ventura, Y. O. N. (1989) *FCTL, Folia Chim. Theor. Lat. 17*, 191–223.
Dannenberg, J. J., & Evlet, E. M. (1992) *Int. J. Quantum Chem. 44*, 864–885.
Dewar, M. J. S., Zoebisch, E. G., Healy, E. F., & Stewart, J. J. P. (1985) *J. Am. Chem. Soc. 107*, 3902–3909.
Dierckx, A. M., Huyskens, P., & Zeegers-Huyskens (1965) *J. Chim. Phys. 62*, 366–344.
Duine, J. A. (1991) *Eur. J. Biochem. 200*, 271–284.
Gacheru, S. N., Trackman, P. C., & Kagan, H. M. (1988) *J. Biol. Chem. 263*, 16704–16708.
Galey, J. B., Bombard, S., Chopard, C., Girerd, J. J., Lederer, F., Do-Cao, T., Nguyen-Hoang, N., Mansuy, D., & Chottard, J. C. (1988) *Biochemistry 27*, 1058–1066.
Grunwald, E. (1965) in *Physical Organic Chemistry* (Cohen, Streitwieser, & Taft, Eds.) Vol. 3, pp 317–358, Wiley, New York.
Hartmann, C., Brzovich, P., & Klinman, J. P. (1993) *Biochemistry 32*, 2234–2241.
Holmgren, A., Lindblom, G., & Johansson, L. B.-Å. (1988) *J. Phys. Chem. 92*, 5639–5642.
Hucko-Haas, J. E., & Reed, D. J. (1970) *Biochem. Biophys. Res. Commun. 38*, 396–400.
Janes, S. M., Mu, D., Wemmer, D., Smith, A. J., Kaur, S., Maltby, D., Burlingame, A. L., & Klinman, J. P. (1990) *Science 248*, 981–987.
Lamkin, M. S., Williams, T. J., & Falk, M. C. (1988) *Arch. Biochem. Biophys. 261*, 72–79.
Lindemann, R., & Zundel, G. (1977a) *J. Chem. Soc., Faraday Trans. II 73*, 788–802; (1977b) *Biopolymers 16*, 2407–2418.
Lobenstein-Verbeek, C. L., Jongejan, J. A., Frank, J., & Duine, J. A. (1984) *FEBS Lett. 170*, 305–309.
Mahy, J. P., Gaspard, S., & Mansuy, D. (1993) *Biochemistry 32*, 4014–4021.
Morozov, Y. V., & Chekhov, V. O. (1989) *Russ. J. Phys. Chem. 63*, 1–22.
Morpurgo, L., Befani, O., Sabatini, S., Mondovi, B., Artico, M., Corelli, F., Massa, S., Stefancich, G., & Avigliano, L. (1988) *Biochem. J. 256*, 565–570.
Morpurgo, L., Agostinelli, E., Muccigrosso, J., Martini, F., Mondovi, B., & Avigliano, L. (1989) *Biochem. J. 260*, 19–25.
Morpurgo, L., Agostinelli, E., Mondovi, B., & Avigliano, L. (1990) *Biol. Met. 3*, 114–117.
Morpurgo, L., Agostinelli, E., Mondovi, B., Avigliano, L., Silvestri, R., Stefancich, G., & Artico, M. (1992) *Biochemistry 31*, 2615–2621.
Mure, M., & Klinman, J. P. (1993) *J. Am. Chem. Soc. 115*, 7117–7127.
Nakamoto, K., Margoshes, M., & Rundle, R. E. (1955) *J. Am. Chem. Soc. 77*, 6480–6486.
Pedersen, J. Z., El-Sherbini, S., Finazzi-Agro, A., & Rotilio, G. (1992) *Biochemistry 31*, 8–12.
Pettersson, G. (1985) in *Structure and Function of Amine Oxidases* (Mondovi, B., Ed.) pp 105–120, CRC Press, Boca Raton, FL.
Sanders-Loehr, J., Backes, G., Kahlow, M. A., Davidson, V. L., Duine, J. A., & Klinman, J. P. (1991) *J. Inorg. Biochem. 43*, 194.
Schuster, P., Zundel, G., & Sandorfy, C., Eds. (1976) *The hydrogen bond*, North Holland, Amsterdam, Vol.s 1–3.
Schwarzenbach, G., & Suter, H. (1941) *Helv. Chim. Acta 24*, 617–638.
Scott, R., De Palma, D., & Vinogradov, S. (1968) *J. Phys. Chem. 72*, 3192–3201.
Tinland, B. (1968) *Theoret. Chim. Acta 12*, 85–86.
Ventura, Y. O. N., Coitiño, E. L., Lledós, A., & Bertránd, J. (1989) *THEOCHEM 187*, 55–68.
Vinogradov, S. M., & Linnell, R. H. (1971) in *Hydrogen Bonding*, Chapters 3, 6, Van Nostrand Reinhold Co., New York.
Williams, T. J., & Falk, M. C. (1986) *J. Biol. Chem. 261*, 15949–15954.